Synthesis and Degradation of Biodegradable Photo-Cross-Linked Poly(α,β-malic acid)-Based Hydrogel

Bin He,† Elsa Wan, and Mary B. Chan-Park*

School of Chemical and Biomedical Engineering, Nanyang Technological University, 50 Nanyang Avenue, 639798 Singapore

Received December 1, 2005. Revised Manuscript Received May 5, 2006

To create a new biodegradable hydrogel, 2-hydroxyethyl methacrylate (HEMA) was grafted on poly(α,β-malic acid) (PMA) and ultraviolet (UV) photo-cross-linked. PMA was synthesized by polycondensation of L-malic acid without catalyst. The effects of the polycondensation reaction time and temperature on the polymer properties were studied. Increased temperature (in the range 110−130°C) accelerated intramolecular dehydration and depolymerization side reactions, increasing the low molecular weight fraction. The intramolecular dehydration was more sensitive to temperature than to reaction time. The photo-cross-link was carried out in the presence of photoinitiator Irgacure 2959. The gel content increased with increasing polymer concentration. The water uptake of PMA-based hydrogel ranged from 170% to 480% as the HEMA content varied from 12 to 4 mol %, respectively. The degradation behavior of PMA-based hydrogel was investigated. The weight loss of hydrogel was closely related to the HEMA grafting content and polymer concentration. Hydrogel degradation was found to proceed simultaneously at the surface and in the bulk of the hydrogels.

1. Introduction

Hydrogels are of great interest to biomaterials scientists because of their hydrophilicity, biocompatibility, and three-dimensional (3-D) microenvironment forming capability.[1] In-situ-forming hydogels have many biomedical applications including tissue engineering,[1] cell-based biosensors,[2] coatings,[3] drug delivery,[4] and cell transplantation.[5] Various techniques for in-situ formation have been investigated.[6−14] Ultraviolet (UV) photopolymerization to form hydrogels using acrylate and its derivatives has many advantages over others,[15,16] offering fast curing rates at room or physiological temperatures, the ability to place the gel in vivo without surgical intervention, minimal heat production, and good gel mechanical properties.

In tissue engineering, hydrogels are fabricated as scaffolds for cell adhesion, spreading, and proliferation. Such scaffolds must degrade as the engineered tissue is formed. Poly(α-hydroxyl acid)s (PHAs) such as poly(lactic acid) (PLA), poly(glycolic acid) (PGA), and poly(ϵ-caprolactone) (PCL) are biodegradable and biocompatible, but their poor hydrophilicity renders them unsuitable for direct use as hydrogels. Many researchers have attempted to modify PHAs for application in biodegradable hydrogels by copolymerization with poly(ethylene glycol) (PEG).[17−19] The nonbiodegradable PEG segment can be eliminated by the kidneys when its molecular weight is less than about 10 000 Da. Formation of biodegradable hydrogels from these copolymers is feasible only when the proportion of PEG to PHAs is high. Hydrophilicity modification of PHAs by ring-opening copolymerization of malolactonate and lactones has been reported,[20−24] but these copolymers are not water soluble and cannot form hydrogels by cross-linking. Some researchers have investigated other biodegradable hydrogels such as hyaluronic acid,[25] poly(L-lysine),[26] and poly(phosphate);[27] despite these

* To whom correspondence should be addressed. Phone: (65) 6790 6064. E-mail: mbechan@ntu.edu.sg.

† Current address: Engineering Research Center in Biomaterials, Sichuan University, Chengdu 610064, China.

(1) Nguyen, K. T.; West, J. L. *Biomaterials* **2002**, *23*, 4307.
(2) Albrecht, D. R.; Tsang, V. L.; Sah, R. L.; Bhatia, S. N. *Lab Chip* **2005**, *5*, 111.
(3) Nakayama, Y.; Kim, J. Y.; Nishi, S.; Ueno, H.; Matsuda, T. *J. Biomed. Mater. Res.* **2001**, *57*, 559.
(4) Peppas, N. A.; Keys, K. B.; Torres-Lugo, M.; Lowman, A. M. *J. Controlled Release* **1999**, *62*, 81.
(5) Elisseeff, J.; McIntosh, W.; Anseth, K.; Riley, S.; Ragan, P.; Langer, R. J. *Biomed. Mater. Res.* **2000**, *51*, 164.
(6) Rydholm, A. E.; Bowman, C. N.; Anseth, K. S. *Biomaterials* **2005**, *26*, 4495.
(7) Peppas, N. A.; Benner, R. E. *Biomaterials* **1980**, *1*, 158.
(8) Ichi, T.; Watanabe, J.; Ooya, T.; Yui, N. *Biomacromolecules* **2001**, *2*, 204.
(9) Gacesa, P. *Carbohydr. Polym.* **1988**, *8*, 161.
(10) Yokoyama, F.; Masada, I.; Shimamura, K.; Ikawa, T.; Monobe, K. *Colloid Polym. Sci.* **1986**, *264*, 595.
(11) Eagland, D.; Crowther, N. J.; Butler, C. J. *Eur. Polym. J.* **1994**, *30*, 767.
(12) Petka, W.; Harden, J.; McGrath, K.; Wirtz, D.; Tirrell, D. A. *Science* **1998**, *281*, 389.
(13) Tang, A.; Wang, C.; Stewart, R. J.; Kopecek, J. *J. Controlled Release* **2001**, *72*, 57.
(14) Miyata, T.; Asami, N.; Uragami, T. *Nature* **1999**, *399*, 766.
(15) Kim, B. S.; Hrkach, J. S.; Langer, R. *Biomaterials* **2000**, *21*, 259.
(16) Vyavahare, N.; Kohn, J. J. *Polym. Sci. Polym. Chem.* **1994**, *32*, 1271.
(17) Li, S. M.; Vert, M. *Macromolecules* **2003**, *36*, 8008.
(18) Behravesh, E.; Jo, S.; Zygourakis, K.; Mikos, A. G. *Biomacromolecules* **2002**, *3*, 374.
(19) Sawhney, A. S.; Pathak, C. P.; Hubbell, J. A. *Macromolecules* **1993**, *26*, 6, 581.
(20) Kimura, Y.; Shirotani, K.; Yamane, H.; Kitao, T. *Macromolecules* **1988**, *21*, 3338.
(21) Kimura, Y.; Shirotani, K.; Yamane, H.; Kitao, T. *Polymer* **1993**, *34*, 1741.
(22) Bizzarri, R.; Chiellini, F.; Solaro, R.; Chiellini, E.; Camamas, S.; Guerin, P. *Macromolecules* **2002**, *35*, 1215.
(23) He, B.; Bei, J. Z.; Wang, S. G. *Polymer* **2003**, *44*, 989.
(24) He, B.; Chan-Park, M. B. *Macromolecules* **2005**, *38*, 8227.

10.1021/cm0526516 CCC: $33.50
Published on Web 07/26/2006

Scheme 1. (a) Chemical Structure of Irgacure 2959, and (b) Synthetic Route of Poly(α,β-malic acid)-Based Hydrogel

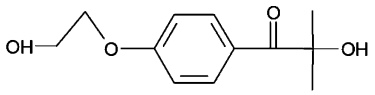

(a)

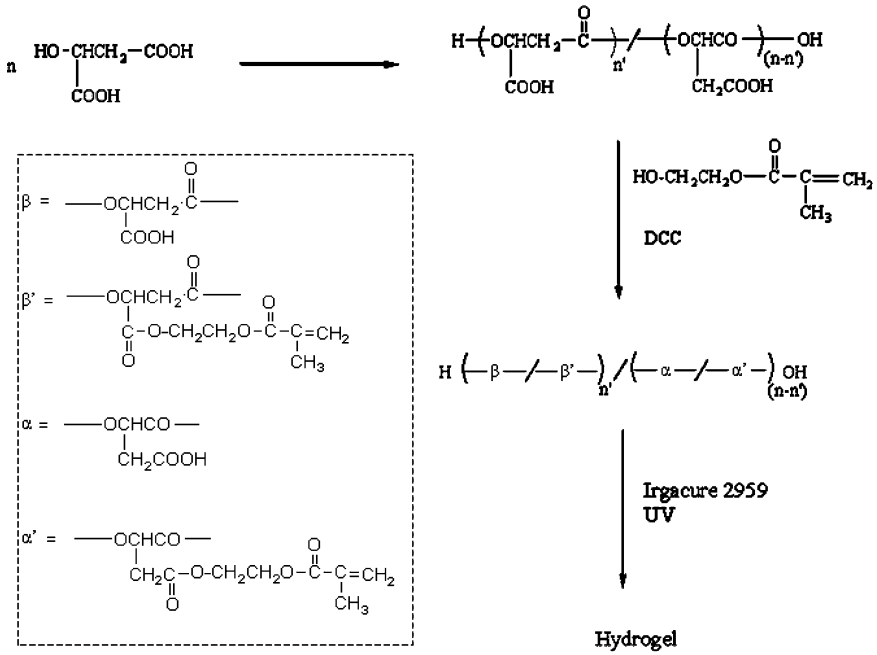

(b)

efforts the range of choices for synthetic biodegradable polyester hydrogels remains limited.

Poly(malic acid) is a biodegradable and water-soluble synthetic polyester.[28−30] It degrades by hydrolysis to malic acid, which is the medial product in the metabolism of carbohydrates and is nontoxic to cells and tissues. Two synthetic routes to poly(malic acid)s with different main-chain structures have been reported. One is ring-opening polymerization of malolactonate to obtain poly(β-malic acid),[28,29] a long, complicated route with low yield. The alternative, reported by Kajiyama et al.,[30] is polycondensation of L-malic acid to yield poly(α,β-malic acid). Though the molecular weight of poly(α,β-malic acid) prepared by polycondensation is typically low (less than 5000 Da), it is a simple way to prepare biodegradable poly(α,β-malic acid)-based hydrogels. The preparation and degradation of poly-(α,β-malic acid)-based hydrogel has not been previously reported.

In this paper we report the preparation and characterization of a new biodegradable hydrogel based on poly(α,β-malic acid). The effects of polycondensation temperature and time on poly(α,β-malic acid) properties were investigated. 2-Hydroxyethyl methacrylate (HEMA) was grafted on poly(α,β-malic acid) (PMA) to provide photo-cross-linkable functionalities. The PMA-*g*-HEMA was UV photo-cross-linked in the presence of water and a photoinitiator to form hydrogel. Formulation effects and hydrogel properties, such as percent of gel content, hydrogel water uptake, and weight loss during degradation, are reported. The degradation mechanism of poly(α,β-malic acid)-based hydrogel is discussed.

2. Experimental Section

Materials. L-Malic acid, *N*,*N*′-dicyclohexylcarbodiimide (DCC), and 2-hydroxyethyl methacrylate (HEMA) were purchased from Aldrich and used as received. The photoinitiator Irgacure 2959 (1-[4-(2-hydroxyethoxy)-phenyl]-2-hydroxy-2-methyl-1-propane-1-one) (Scheme 1a) was purchased from Ciba. Tetrahydrofuran (THF) and diethyl ether were dried by refluxing over sodium and distilled under a nitrogen atmosphere. Phosphate-buffered saline was purchased from Fluka.

Synthesis of PMA. A 50 g amount of L-malic acid was added in a 100 mL bottom-round flask with a magnetic stirrer. The polycondensation was carried out under 0.1 mmHg vacuum with nitrogen protection for several hours. Multiple reactions were performed at temperatures of 110, 120, and 130 °C. The polymerized products were dissolved in anhydrous THF and precipitated in a large amount of diethyl ether. The diethyl ether was removed, and the remaining white precipitate, PMA, was vacuum-dried at room temperature for 24 h.

HEMA-Grafted PMA (PMA-*g*-HEMA). HEMA was grafted onto PMA in proportions ranging from 4 to 12 mol %. The

(25) Leach, J. B.; Bivens, K. A.; Patrick, C. W.; Schmidt, C. E. *Biotechnol. Bioeng.* **2003**, *82*, 578.
(26) Yamamoto, H.; Kitsuki, T.; Nishida, A.; Asada, K.; Ohkawa, K. *Macromolecules* **1999**, *32*, 1055.
(27) Ng, C. C.; Cheng, Y. L.; Pennefather, P. S. *Macromolecules* **2001**, *34*, 5759.
(28) Ouchi, T.; Fujino, A. *Makromol. Chem.* **1989**, *190*, 1523.
(29) Cammas, S.; Renard, I.; Lanhlois, V.; Guerin, P. *Polymer* **1996**, *37*, 4215.
(30) Kajiyama, T.; Kobayashi, H.; Taguchi, T.; Kataoka, K.; Tanaka, J. *Biomacromolecules* **2004**, *5*, 169.

procedure described here is for 4 mol %. A 0.52 g amount of HEMA and 1.24 g of DCC (1:1.5) were added in a 100 mL bottom-rounded flask with 11.8 g of dried PMA and 60 mL of anhydrous THF. The mixture was magnetically stirred at room temperature for 24 h, and white precipitates appeared in the mixture. The mixture was filtered; the filtrate was condensed and precipitated in a large amount of diethyl ether. The purified PMA-*g*-HEMA was vacuum-dried at room temperature for 24 h.

UV Photo-Cross-Linking. PMA-*g*-HEMA was dissolved in distilled water with 2 wt % (to polymer weight) photoinitiator Irgacure 2959. The PMA-*g*-HEMA solution was degassed and purged with nitrogen three times. The PMA-*g*-HEMA solution was photo-cross-linked to form a hydrogel under 365 nm UV irradiation with intensity 16 mW/cm^2 for 90 s. The photo-cross-linking UV lamp was PK102 from I & J Fisnar Inc.

Percent Polymer Gel Content. The percent polymer gel content was determined as the dry weight ratio of PMA-based hydrogel after water extraction of unreacted polymer to the initial PMA-*g*-HEMA polymer used. The hydrogel was put into a 100 mL beaker with 50 mL of distilled water and violently stirred for 30 min to break the hydrogel into particles. The mixture was filtered and washed twice with distilled water. The particles were vacuum-dried and weighed to calculate the percent polymer gel content. Five parallel samples of each hydrogel were measured to calculate the average values.

$$\text{percent polymer gel content} = \frac{\text{weight of dried hydrogel after extraction}}{\text{weight of initial dried polymer}} 100$$

Water Uptake Measurement. The hydrogel was washed with distilled water to remove the un-cross-linked PMA-*g*-HEMA and dipped into distilled water for 10 min. Free water on the surface of the hydrogel was absorbed with filter paper, and the gel was then weighed. The hydrogel was then freeze-dried and again weighed. Five parallel samples of each hydrogel were measured to calculate the average value. The water uptake was calculated as

$$\text{water uptake percent} = 100x\frac{\text{wet hydrogel weight} - \text{hydrogel dry weight}}{\text{hydrogel dry weight}}$$

Hydrogel Degradation. Each photo-cross-linked hydrogel sample was put in a 50 mL beaker with 20 mL of pH 7.4 phosphate buffer solution (PBS). The beakers were put in a shaking bed and agitated at 50 cycles/min at 37 °C. The PBS was changed every 24 h. The degraded hydrogel samples were washed three times with distilled water; then they were freeze-dried and weighed. Five parallel samples of each degraded hydrogel were measured. The weight remaining was calculated as

$$\text{weight left percent} = 100x\frac{\text{degraded hydrogel dry weight}}{\text{initial hydrogel dry weight}}$$

Characterization. The solvent for ^{1}H NMR measurement was D_2O with 0.5% tetramethylsilane as the internal standard. ^{1}H NMR spectra were recorded on a Bruker DMX-300 spectrometer, working at 300.130 MHz. FTIR spectra were recorded on a Nicolet 560 spectrometer over the wavenumber range 4000−400 cm^{-1}. Number- and weight-average molecular weights (M_n and M_w, respectively) and the polydispersity (M_w/M_n) were determined by gel permeation chromatography (GPC) with respect to polystyrene standards. GPC was performed on an Agilent 1100 Series and analyzed with GPC−SEC (size exclusion chromatography) data analysis software. Samples were analyzed at 25 °C with tetrahydrofuran as eluent at a flow rate of 1.0 mL min^{-1}. Differential scanning calorimetry (DSC) was performed on a TA System Q10; the sample was first heated to 120 °C, then cooled to −30 °C, and heated again to 120 °C with 10 °C/min heating and cooling rates in a nitrogen environment. Freeze-drying was carried out in a Christ freeze-dry machine (Alpha1-2) at −60 °C and 0.012 mbar pressure. The morphologies of dry hydrogel samples were observed with SEM (Joel JSM-5600 at 10 kV). Pictures of hydrogel samples were taken with a Canon digital camera (Canon A80).

Table 1. Polycondensation of L-Malic Acid

entry	temp (°C)	time (h)	molecular weight M_n[a]	M_n[b]	M_w[a]	M_w[b]	M_w/M_n[a]	M_w/M_n[b]	yield[c] (%)
1	110	15	570	1150	900	1640	1.58	1.43	20
2	110	24	700	1540	1150	2290	1.64	1.49	29
3	110	36	760	1640	1350	2330	1.78	1.42	46
4	110	48	990	1830	1840	2560	1.85	1.40	47
5	110	60	1210	2280	2376	3150	1.97	1.38	53
6	110	70	1380	2250	2800	3220	2.03	1.43	51
7	120	24	1000	1870	2330	2510	2.32	1.34	43
8	120	48	830	2040	2370	2670	2.85	1.31	49
9	120	72	810	2010	2420	2650	2.99	1.32	39
10	130	24	730	2200	2130	3000	2.92	1.35	43
11	130	48	690	2150	2070	2830	3.01	1.31	35

[a] GPC results including all peaks. [b] GPC results of the main peak. [c] Yield after precipitation in diethyl ether.

3. Results and Discussion

The synthetic route of PMA-*g*-HEMA is presented in Scheme 1b. The first step was to synthesize poly(α,*β*-malic acid), which was carried out by polycondensation of L-malic acid without catalyst. This reaction is much simpler than the alternative, ring-opening polymerization of malolactonate to yield poly(malic acid). As there was no selection for α or *β* type of L-malic acid units in aggregation, both α and *β* types were reacted randomly in polycondensation, denoted by units, α,α′ and *β*,*β*′, respectively, as described in the figure inset. HEMA was grafted on the pendant groups of poly(α,*β*-malic acid) and UV photo-cross-linked in the presence of water and a photoinitiator to form PMA-based hydrogel.

The molecular weights of poly(α,*β*-malic acid)s produced under various reaction parameters are shown in Table 1. As all the GPC spectra of poly(α,*β*-malic acid) were multiply peaked, we analyzed the GPC results to produce two measures of molecular weight and polydispersity: one includes all the peaks, and the other considers the main peak only. We select the second measurement, which is derived from the main and high molecular weight fragment, to discuss the effects of temperature and time on polycondensation reaction outcomes. The polycondensation of L-malic acid was performed at reaction temperatures and times ranging from 110 to 130 °C and 15 to 72 h, respectively. The M_n, M_w, and polydispersity (using only the main peak) of poly(α,*β*-malic acid) under these conditions range from 1150 to 2280, 1640 to 3220, and 1.31 to 1.49, respectively. The yield after precipitation in diethyl ether is from 20% to 53%.

In the 110 °C series PMA samples both M_n and M_w generally increase with increasing polycondensation time. The weight-average molecular weight (M_w) in this series is maximal at the longest tested reaction time, 70 h; we cannot rule out that it may increase further at longer reaction times. The yield increases roughly linearly to 46% at 36 h, after which it plateaus at around 50%. The yield trend with time

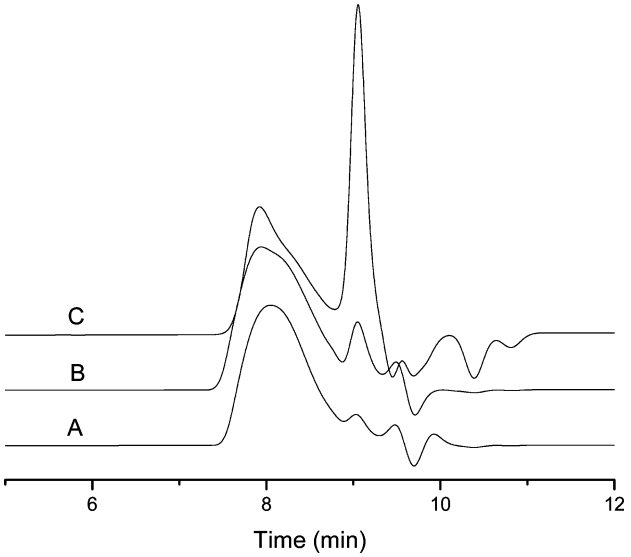

Figure 1. GPC spectra of L-malic acid polycondensation at different temperatures for 48 h: (A) 110 °C (entry 4), (B) 120 °C (entry 8), and (C) 130 °C (entry 11).

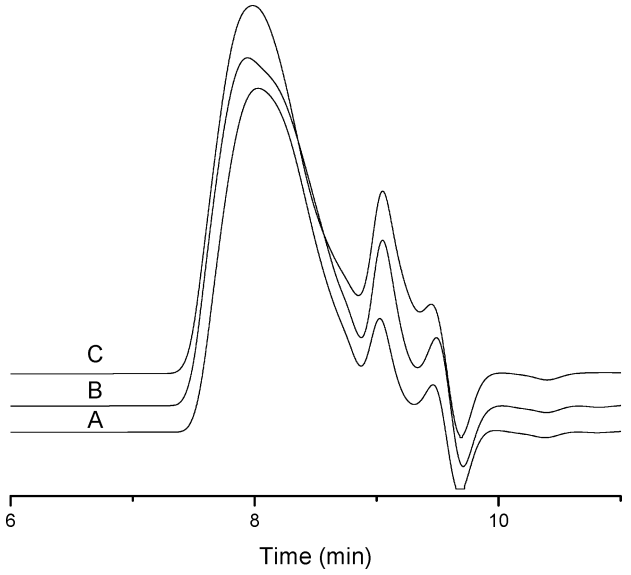

Figure 2. GPC spectra of L-malic acid polycondensation at 120 °C for different times: (A) 24 h (entry 7), (B) 48 h (entry 8), and (C) 72 h (entry 9).

is accounted for by the sequential nature of polycondensation: the low molecular weight fragments formed early in the reaction are more soluble in diethyl ether, suppressing the yield, while the higher molecular weight fragments formed at longer reaction times are less soluble. In the 120 and 130 °C series the changes of M_n, M_w, and polydispersity are not as regular as those of the 110 °C series. The weight-average molecular weight (M_w) in the 130 °C series decreases at the longer tested reaction time. These results show that the polycondensation reaction outcomes are sensitive to both the reaction temperature and duration.

To study the effect of temperature on the reaction, a series of polycondensations was carried out at different temperatures for 48 h. The GPC spectra are shown in Figure 1. The low molecular weight fragment peak at 110 °C (entry 4) is very small, enlarges when the temperature was increased to 120 °C (entry 8), but is still much smaller than the main peak. At 130 °C, it enlarges significantly to be much higher

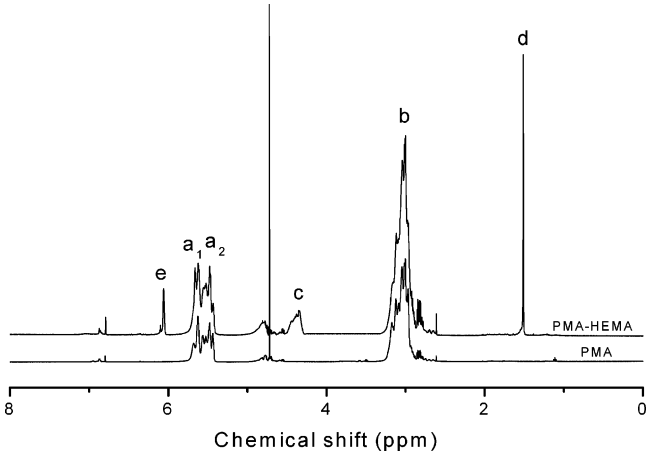

Figure 3. ^{1}H NMR spectra of PMA synthesized at 110 °C for 70 h (entry 6) and its corresponding PMA-*g*-HEMA (12 mol %) (asterisk indicates D_2O as solvent.)

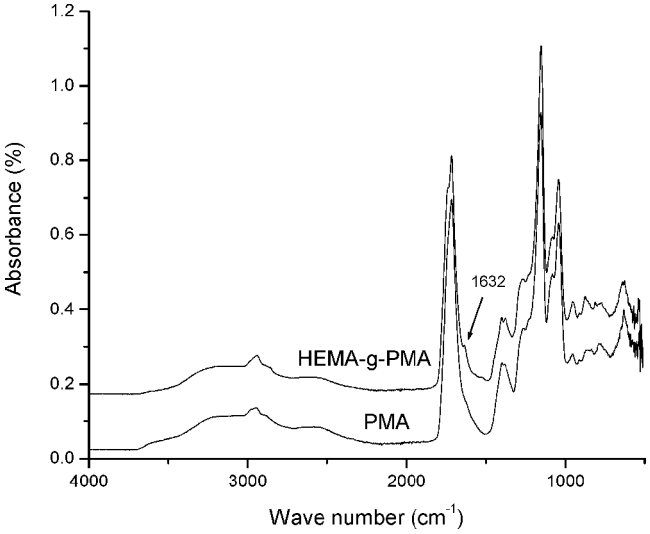

Figure 4. FTIR spectra of PMA (entry 6) and PMA-*g*-HEMA (12 mol %).

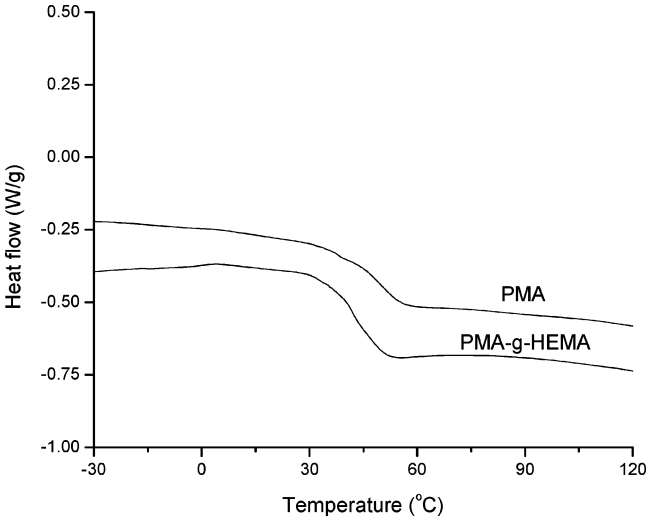

Figure 5. DSC spectra of PMA (entry 6) and PMA-*g*-HEMA (12 mol %).

than the main peak, indicating that at this temperature side reactions, which reduce molecular weight, are accelerated greatly. The possible side reactions of polycondensation are depolymerization and intramolecular dehydration of L-malic acid.[30] From the spectra of Figure 1 we conclude that side

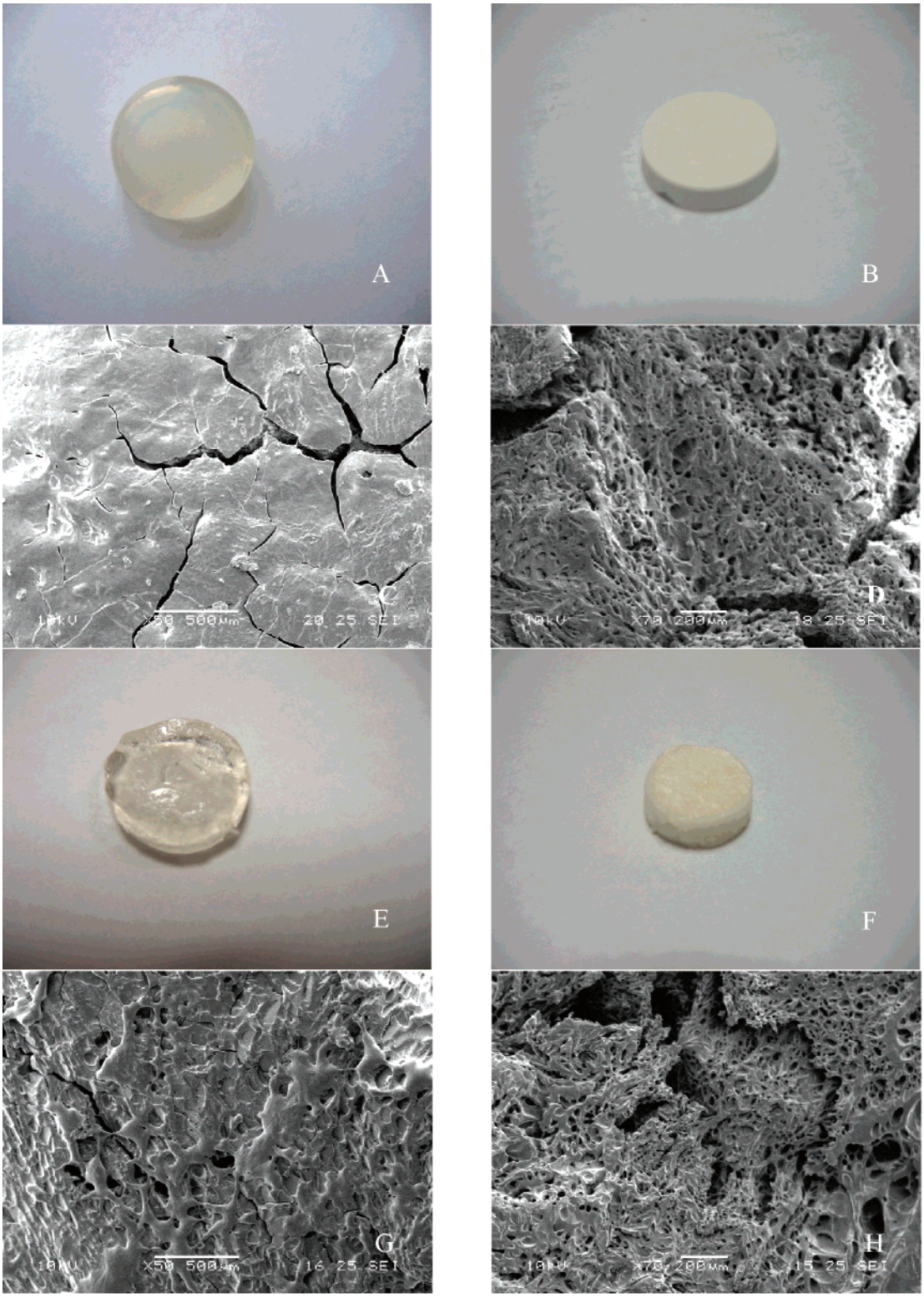

Figure 6. Pictures of PMA-*g*-HEMA (12 mol %) hydrogel: (A) 50 wt % polymer, (B) freeze-dried A, (C) SEM surface of B, (D) SEM cross-section of B, (E) 20 wt % polymer, (F) freeze-dried E, (G) SEM surface of F, and (H) SEM cross-section of F.

reactions are greatly accelerated as the polycondensation temperature increases from 110 to 130 °C.

Reaction time also affects the polycondensation. GPC spectra of PMA synthesized at 120 °C for 24, 48, and 72 h (entries 7, 8, and 9) are shown in Figure 2. All the spectra have three peaks. The intensity of the low molecular weight peak increases with increasing time (at least between 24 and 48 h) but not as dramatically as the temperature effect discussed above. The side reactions continue between 24 and 48 h but seem to saturate beyond 48 h. The side reactions of depolymerization and intramolecular dehydration of L-malic acid are much more sensitive to reaction temperature than to reaction time. Longer reaction time at lower temperature is more favorable for synthesizing PMA with higher molecular weight. PMA (entry 6) was used in subsequent experiments.

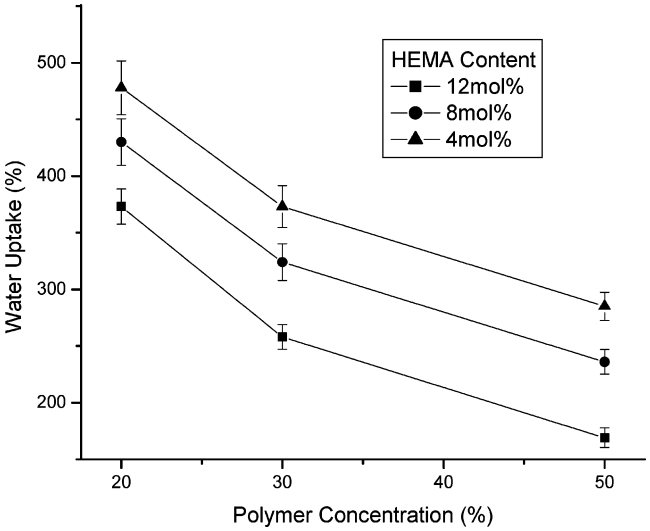

Figure 7. Water uptake of PMA-*g*-HEMA hydrogels with HEMA grafting contents of 12, 8, and 4 mol % plotted against polymer concentrations (20, 30, and 50 wt %).

^{1}H NMR spectra of PMA and its corresponding PMA-*g*-HEMA (12 mol %) are presented in Figure 3. The peaks at 6.1, 4.4, and 1.5 ppm are assigned to protons in HEMA, which are C═CH_2 (e), CH_2CH_2 (c), and CH_3 (d), respectively. The multipeaks at 3.0−3.2 ppm are the protons of CH_2 (b) in both *β* and α type L-malic acid units. The random aggregation of α and *β* type of L-malic acid in the main chain and the small difference in the chemical environment of these protons cause the signals of these protons to split into multipeaks. The double peaks at 5.6 and 5.5 ppm are attributed to the protons of C*H* in the poly(α,*β*-malic acid) backbone; the peak at 5.6 ppm is *β* type (a_1), whereas that at 5.5 ppm is α type (a_2). The two peaks are of nearly equivalent intensity, implying that the sequences of *β*- and α-type units in the polymer are present in near-identical ratios. The wide peak at around 4.7 ppm is attributed to both to the ^{1}H NMR solvent D_2O and the terminal hydroxyl hydrogen. The small peaks at around 6.8 ppm are olefinic hydrogen attributed to fumaric acid, which is an intramolecular dehydration product. The intensity of this peak increased more rapidly with temperature than with reaction time, providing further evidence that the intramolecular dehydration side reaction is more sensitive to temperature than to time. From intensity ratios between CH_3 (d) in HEMA and C*H* (a_1 and a_2) in poly(α,*β*-malic acid) backbone, we calculated the grafting content of HEMA and found it to be nearly the same as that in the feeding dose.

FTIR spectra of the same PMA and PMA-*g*-HEMA are shown in Figure 4. The two spectra are nearly the same except that a new shoulder at 1632 cm^{-1} appears in the PMA-*g*-HEMA spectrum, which is the characteristic vibration of C═C in HEMA. The wide band from 3500 to 2500 cm^{-1} is the vibration of carboxyl groups; it weakens slightly after HEMA grafting. The FTIR spectra confirm the grafting of HEMA onto the pendant groups of PMA.

DSC spectra of PMA and PMA-*g*-HEMA are shown in Figure 5. Both PMA and PMA-*g*-HEMA are amorphous polymers. The glass transition temperatures (T_g) of PMA and PMA-*g*-HEMA (12 mol %) are 50 and 42 °C, respectively.

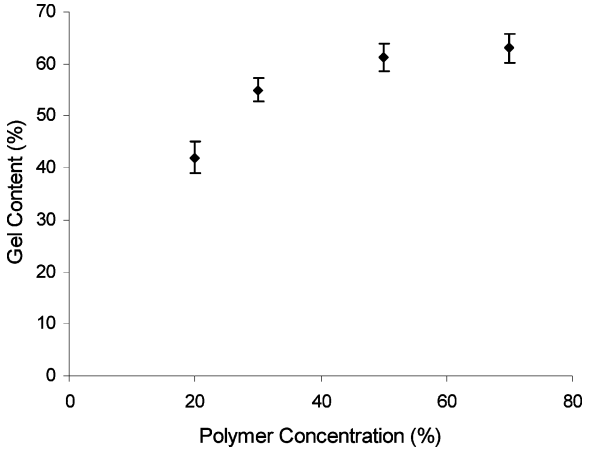

Figure 8. Polymer gel content of PMA-*g*-HEMA (8 mol %) hydrogel versus polymer concentration.

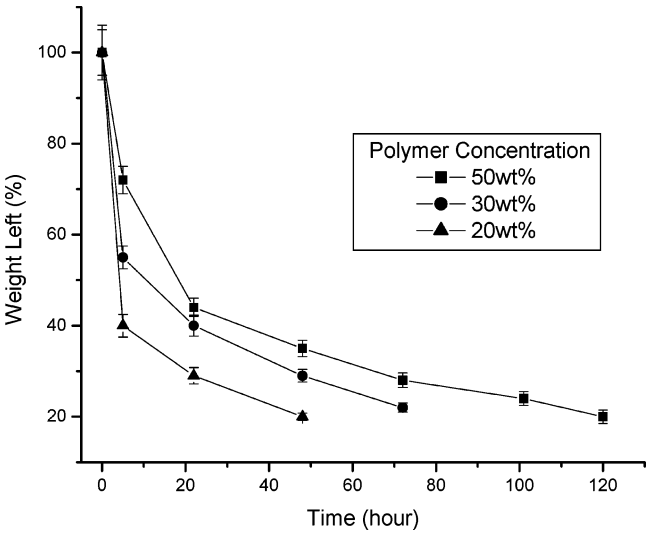

Figure 9. Weight loss of PMA-*g*-HEMA (8 mol %) hydrogel samples agitated in PBS versus immersion time (the three curves are for different polymer concentrations). The last point is the last measured time before the hydrogel lost its shape.

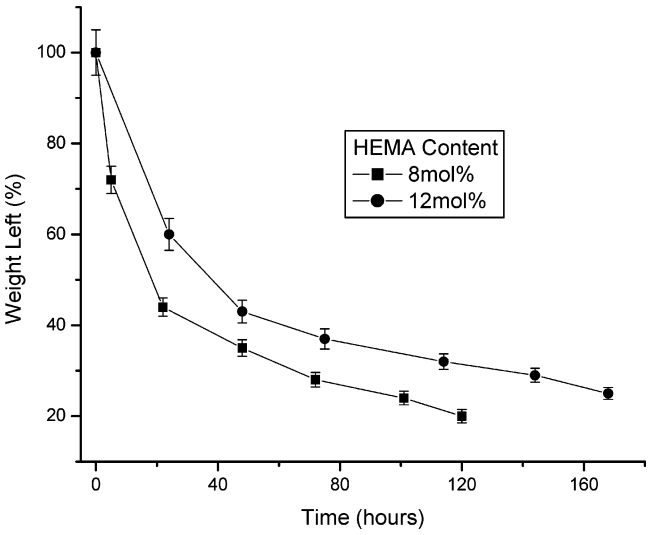

Figure 10. Weight loss of PMA-*g*-HEMA (50 wt % polymer concentration) hydrogel samples in PBS versus immersion time.

The T_g of PMA-*g*-HEMA is lower than that of PMA and decreases monotonically with increasing HEMA content: the T_g varied from 47 to 45 °C as the HEMA grafting content

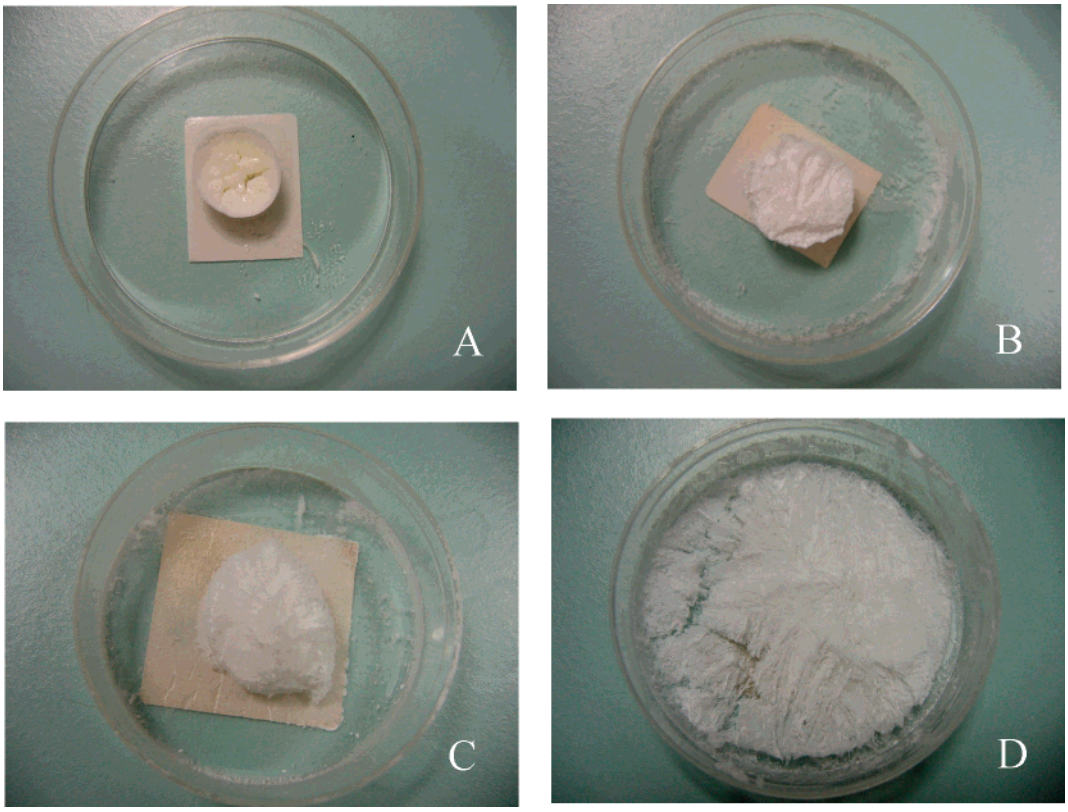

Figure 11. Shapes of freeze-dried hydrogel samples in degradation (12% HEMA and 50 wt % polymer content): (A) origin, (B) 3 days, (C) 5 days, and (D) 7 days.

increased from 4 to 8 mol %, respectively. This trend is due to a weakening of hydrogen-bond interactions between pendant groups caused by the grafting of HEMA.

Hydrogels were formed by UV photo-cross-linking of PMA-*g*-HEMA water solutions. Pictures of the hydrogels are shown in Figure 6. Samples A and E are water-swollen PMA-*g*-HEMA (12 mol %) hydrogels with 50 and 20 wt % polymer dry weight, respectively. Samples B and F are A and E after freeze-drying. C and G are SEM pictures of the surfaces of samples B and F, respectively. D and H are cross-sectional SEM pictures of samples B and F. The shape of sample A is well preserved, and its surface is smooth. The surface of sample E is dented. Both samples A and E are transparent. After freeze-drying (Figure 6B and F), both samples shrank substantially (10% and 40% volume shrinkage, respectively) because of removal of water. SEM indicates that both of the samples are porous in cross-section, but there are very few pores on the sample B surface (Figure 6C) and some pores on the sample F surface (Figure 6G). The number and size of pores in sample F were observed to be much higher than that of sample B because the water content in sample E (80 wt %) is much higher than that in sample A (50 wt %).

Hydrogels can absorb a large amount of water into their cross-linked net structure. There are three kinds of water in hydrogels: primary bound water, secondary bound water, and free water. The primary and secondary bound water are often combined and simply called the total bound water. The total bound water is the water interacting with the polar, hydrophilic, and hydrophobic groups in hydrogel. The free water is assumed to fill the space between the network chains and/or the centers of larger pores, macropores, or voids.[31] Water uptake encompasses all three kinds of water in a hydrogel. The water uptake of our PMA-*g*-HEMA hydrogels is presented in Figure 7. The water uptake decreases with increasing HEMA content. For example, the water uptake is as high as 480% in the hydrogel with 4 mol % HEMA content; it decreases to 440% at 8 mol % and to 380% at 12 mol %. The water uptake also decreased with increasing polymer concentration; for example, the water uptake of PMA-*g*-HEMA (12 mol %) is 380%, 260%, and 170% with corresponding polymer concentration of 20, 30, and 50 wt %. The cross-linking density in a hydrogel is the average molecular weight between two cross-link sites and affected in our hydrogels by HEMA content. High HEMA content increases the cross-linking density (as also observed in other hydrogels with pendant functionalities [32,33]), thus lowering the water uptake. When the polymer concentration increases, the polymer occupies more space in the hydrogel, again decreasing the water uptake potential.

When photo-cross-linking is carried out in a polymer water solution it is hard to cross-link all the grafted HEMA. The fraction of PMA-*g*-HEMA cross-linked into the gel was determined by weighing the filtered gel particles after removal of soluble un-cross-linked polymer (Figure 8). The percent polymer gel content increases with increasing polymer concentration from 42% to 55% to 62% at polymer concentrations of 20, 30, and 50 wt %, respectively. We find

(31) Hoffman, A. S. *Adv. Drug Delivery Rev.* **2002**, *54*, 3.
(32) Cadee, J. A.; de Groot, C. J.; Jiskoot, W.; den Otter, W.; Hennink, W. E. *J. Controlled Release* **2002**, *78*, 1.
(33) Lee, W. F.; Chen, Y. J. *J. Appl. Polym. Sci.* **2001**, *81*, 2888.

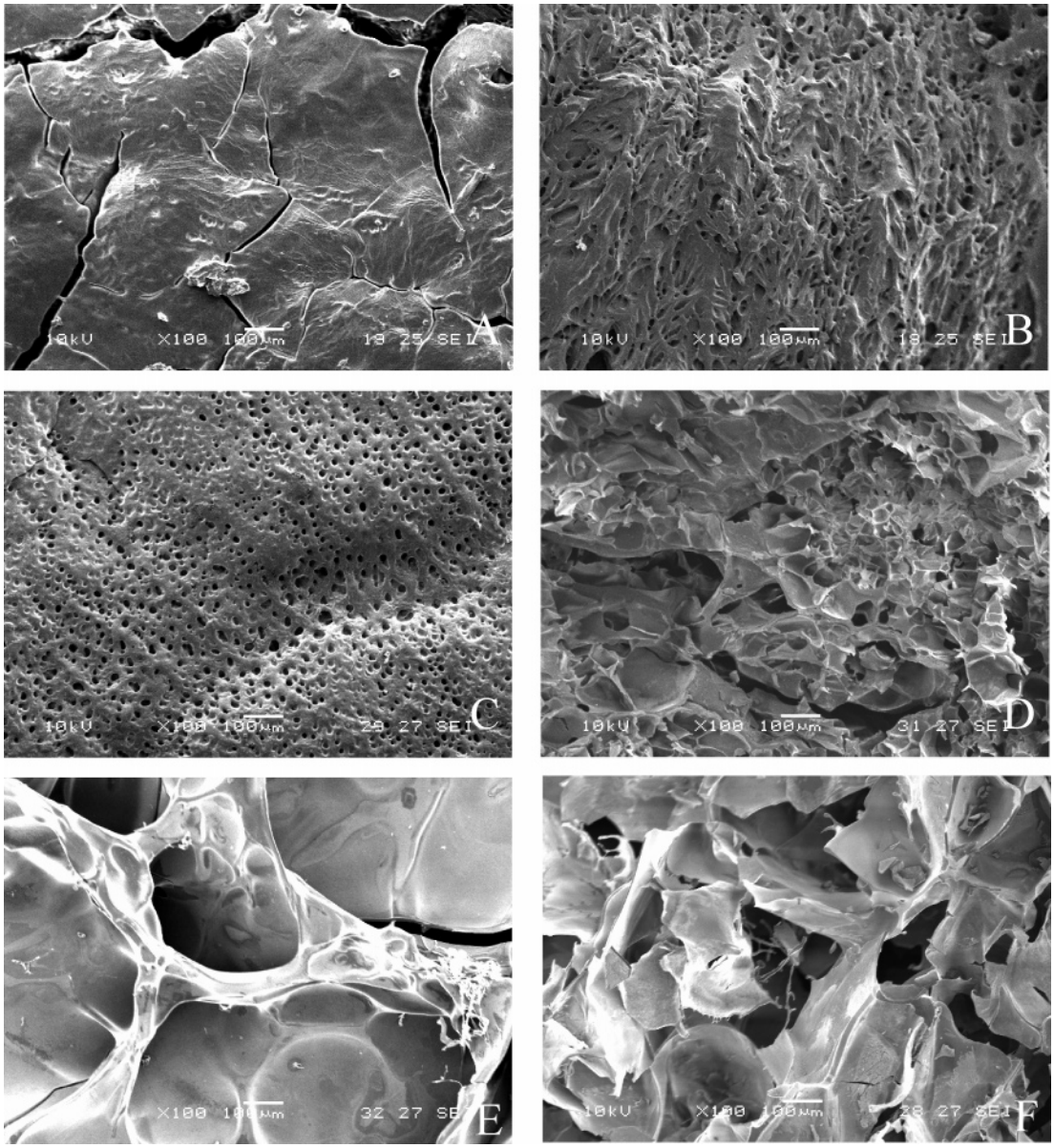

Figure 12. SEM of degraded hydrogel samples (12% HEMA and 50 wt % polymer concentration): (A) surface of origin, (B) cross-section of origin, (C) surface of 3 days, (D) cross-section of 3 days, (E) surface of 5 days, and (F) cross-section of 5 days.

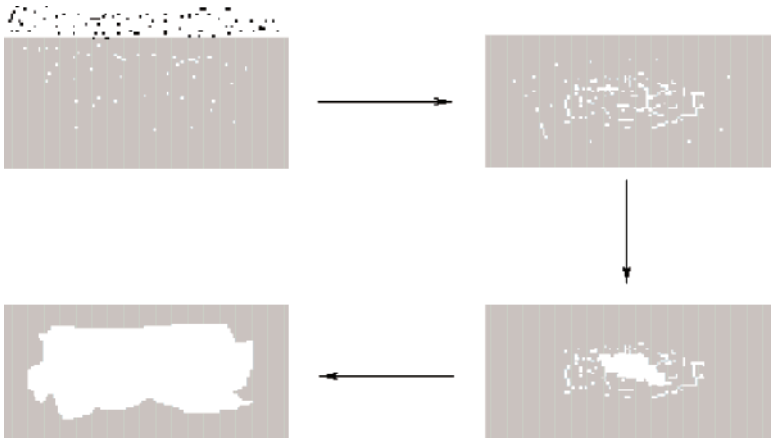

Figure 13. Model of bulk degradation mechanism.

the percent polymer gel content does not increase further even when the polymer concentration is as high as 70 wt %. We interpret this plateau to be due to the limited mobility/restricted diffusion of the polymer chains in the densely cross-linked network that is produced at high HEMA concentration.

The degradation of PMA hydrogels was carried out in PBS at 37 °C. The weight loss of hydrogels with 8 mol % HEMA

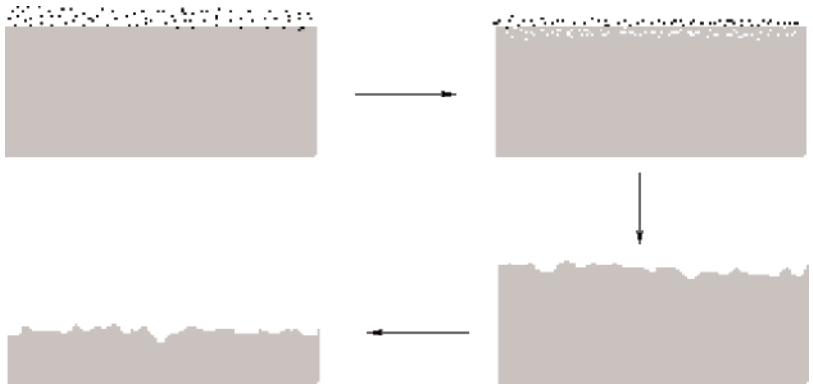

Figure 14. Model of surface degradation mechanism.

grafting prepared in 20, 30, and 50 wt % polymer concentrations is shown in Figure 9. The 20 wt % hydrogel sample degraded completely in 2 days, but the 30 and 50 wt % hydrogel samples lasted for 3 and 5 days. The 20 and 30 wt % hydrogel samples lost 60% and 45% of their weight within the first 5 h, and the weight loss proceeded linearly thereafter. The 50 wt % sample lost 56% of its weight within the first 20 h and degraded linearly thereafter. The weight loss at the last plotted points in Figure 9, about 80%, does not represent the completely degraded state of the samples as samples more degraded than this are like viscous liquids and could not be removed intact from the PBS media to be dried and weighed. The rapid weight loss of the samples in the first several hours is probably due to diffusion of un-cross-linked polymeric chains from inside the hydrogel into the PBS media. The greater the degree of cross-linking in the gel, the harder it is for unreacted polymer chains to diffuse through the hydrogel net to the external environment; this is especially evident in the samples made with 50 wt % polymer concentration.

The degradation of hydrogels with 8 and 12 mol % HEMA is shown in Figure 10. Both hydrogels had 50 wt % polymer concentration. The weight loss of hydrogel with 12 mol % HEMA is slower than that of hydrogel with 8 mol % HEMA. The degradation of 12 mol % HEMA hydrogel lasts for 7 days, which is longer than the 5 days degradation time of hydrogel with 8 mol % HEMA. The weight loss of hydrogel with 12 mol % HEMA is only 40% in the first 20 h. After 48 h, the degradation proceeds with linear weight loss. The increased HEMA content increases the cross-link density and slows the diffusion of un-cross-linked and degraded chains and thus delays the onset of the linear weight loss regime.

The shapes of freeze-dried hydrogel samples (12 mol % HEMA) during the degradation process are shown in Figure 11. The samples enlarge greatly during degradation and do so progressively with the passage of time. After 7 days of degradation, this gel could not retain its scaffold shape in freeze-drying and crumbled. SEM images of the same degraded hydrogel samples are shown in Figure 12. In the original sample there were only cracks in the surface and many small pores in cross-section (Figure 12A and B). After 3 days of degradation, many small pores and cracks appeared in the hydrogel surface (Figure 12C). The pores and cracks also appeared in the cross-section at this degree of degradation (Figure 12D). After 5 days of degradation, the pores and cracks had enlarged in both the surface and cross-section (Figure 12E and F). The whole sample became a three-dimensional porous scaffold.

Two types of degradation mechanisms have been reported in biodegradable polymers: bulk and surface mechanisms.[34,35] The degradation of polyester occurs principally by the bulk mechanism; this is illustrated in Figure 13. When the biodegradable polyester sample contacts with water, the water penetrates into the sample. The polyester hydrolyzes in the presence of water both on the surface and in bulk. As the degradation on the surface is slow and the diffusion of degradation products in bulk is also slow, the interior of the sample becomes acidic. With the self-catalysis effect, the inside degradation rate is much faster than that on the surface and a hole eventually appears inside the polyester sample. By contrast, the surface degradation mechanism is very different. The surface degradation occurs on the surface first and water penetrates inside at the same time. As the surface degradation is very fast, there is no acidity accumulation and self-catalysis. The surface degradation continues layer by layer till the sample is completely degraded (Figure 14). The degradation of polyanhydrides occurs via this mechanism.

From the SEM results, we know that during the degradation of PMA-based hydrogels, pores appear throughout the sample interiors as well as on their surfaces. These pores enlarge and interconnect as the degradation proceeds. This indicates that the hydrogels degrade in the bulk as well as on the surface. The penetration of water into and the diffusion of degradation products out of PMA hydrogels occur much more rapidly than the corresponding processes in the degradation of biodegradable polyester because of the three-dimensional net structure of the hydrogel. There is little acidity contrast between interior and exterior. The localized self-catalysis effect is very weak or absent, so the bulk and surface degrade simultaneously.

Conclusion

We prepared a novel biodegradable PMA-based hydrogel with tunable properties (i.e., biodegradation rate and water

(34) Li, S. M.; Vert, M. Biodegradation of Alphatic Polyesters. In *Biodegradation of Aliphatic Polyesters in Degradable Polymers Principles and Applications*; Scott, G., Gilead, D., Eds.; Chapman & Hall: New York, 1995.

(35) Shakesheff, K. M.; Davies, M. C.; Domb, A.; Jackson, D. E.; Roberts, C. J.; Tendler, S. J. B.; Williams, P. M. *Macromolecules* **1995**, *28*, 1108.

absorption) by UV photo-cross-linking of HEMA grafted PMA. The hydrogel precursor polymer was synthesized by direct polycondensation of L-malic acid, which offers a simple procedure for creation of biodegradable hydrogel precursor. The pendant carboxyl groups in PMA were partially reacted with HEMA to produce PMA-*g*-HEMA, which was photopolymerized in water to produce swollen hydrogels. The water uptake of the hydrogels increases with decreasing HEMA grafting content and polymer concentration and, for the formulations tested, ranges from 170% to 480%. The degradation time of the hydrogels can be controlled from 2 to 7 days. The degradation of PMA-based hydrogels occurs simultaneously on the surface and in bulk.

Acknowledgment. This research was supported by an A-STAR (Singapore) grant (Project No. 022 107 0004).

CM0526516